

Dark Matter, Sparticle Spectroscopy and Muon $(g - 2)$ in $SU(4)_c \times SU(2)_L \times SU(2)_R$

M. E. Gómez,^a S. Lola,^{b,c} R. Ruiz de Austri,^d Q. Shafi^e

^a*Departamento de Física Aplicada, Facultad de Ciencias Experimentales, Universidad de Huelva, 21071 Huelva, Spain*

^b*Institute of Nuclear and Particle Physics, NCSR Demokritos, Agia Paraskevi, 15310, Greece*

^c*on leave from Department of Physics, University of Patras, 26500 Patras, Greece*

^d*Instituto de Física Corpuscular, IFIC-UV/CSIC, Valencia, Spain*

^e*Bartol Research Institute, Department of Physics and Astronomy, University of Delaware, Newark, DE 19716, USA*

E-mail: mario.gomez@dfa.uhu.es, magda@physics.upatras.gr,
r Ruiz@ific.uv.es, shafi@bartol.udel.edu

ABSTRACT: We explore the sparticle mass spectra including LSP dark matter within the framework of supersymmetric $SU(4)_c \times SU(2)_L \times SU(2)_R$ (422) models, taking into account the constraints from extensive LHC and cold dark matter searches. The soft supersymmetry-breaking parameters at M_{GUT} can be non-universal, but consistent with the 422 symmetry. We identify a variety of coannihilation scenarios compatible with LSP dark matter, and study the implications for future supersymmetry searches and the ongoing muon $g-2$ experiment.

Contents

1	Introduction	1
2	The $SU(4)_c \times SU(2)_L \times SU(2)_R$ model	2
3	Exploring the model: Methodology	3
4	Results of the parameter space scan	5
4.1	GUT inputs and Planck compatible regions	7
4.2	Higgs mass and Muon ($g - 2$)	9
4.3	Dark Matter Searches	11
5	LHC searches	12
6	Conclusions	16

1 Introduction

In recent years, a large body of experimental data, including Higgs boson measurements [1, 2] and cosmological observations [3–6], have provided increasingly strong constraints on new physics beyond the Standard Model (SM). Nonetheless, some new physics is required to explain, for instance, the observed solar and atmospheric neutrino oscillations, provide a plausible dark matter (DM) candidate, explain the observed baryon asymmetry in the universe, help understand electric charge quantization, etc.

Among the many plausible SM extensions, supersymmetric theories have several theoretical advantages, including a compelling explanation of the origin of DM through the lightest supersymmetric particle (LSP) [7, 8], and amelioration of the well-known fine tuning problem. Despite the fairly strong LHC [9, 10] and DM [11–16] constraints on supersymmetry (SUSY), there still remain several viable possibilities [17–24]. In this paper we investigate a class of supersymmetric models based on the gauge symmetry $SU(4)_c \times SU(2)_L \times SU(2)_R$ (422) [25–27], which have several interesting features. Electric charge quantization is built in, neutrinos have non-zero masses via the see-saw mechanism, and the observed baryon asymmetry can be explained via leptogenesis. Furthermore, the MSSM μ problem is readily resolved [28] in 422, and inflation can also be nicely implemented [29].

Because of its gauge structure, the 422 model naturally allows one to consider non-universal soft SUSY breaking masses at M_{GUT} for the gluino and scalar sectors, leading to significant differences from other GUTs (Grand Unified Theories). Note also that left-right symmetry may not hold at M_{GUT} . We explore the implications for particle spectroscopy focusing, mostly, on the yet to be found supersymmetric partners of the SM particles, as

well as LSP DM. We identify a variety of coannihilation scenarios that are compatible with the current searches at the LHC and the presence of primordial LSP DM. In addition, supersymmetric contributions to the anomalous magnetic moment of the muon ($g - 2$) could help explain the discrepancy between the SM prediction and the experimental value [30]. In particular, we identify models and SUSY mass relations for which the neutralino relic density is consistent with the cosmological bounds and explore how their parameter space is constrained by the LHC data. These predictions will be tested by the ongoing and future DM and LHC searches.

2 The $SU(4)_c \times SU(2)_L \times SU(2)_R$ model

We start by briefly reviewing the salient features of the 422 model [25, 27], which shares many features, but also shows fundamental differences from standard GUTs such as $SU(5)$ and $SO(10)$. The 422 gauge symmetry can be obtained from a spontaneous breaking of $SO(10)$ by utilizing either the 54 dimensional or the 210 dimensional representation. The breaking of $SO(10)$ with a Higgs 54-plet yields two connected components, namely the 422 subgroup and $\Sigma_{67}.422$, where Σ_{67} is a rotation by π in the 6-7 plane [31, 32].

Instead of Σ_{67} , we could alternatively use the rotation C given by $C = (\Sigma_{23})(\Sigma_{67})$, which is also an element of $SO(10)$. This C -transformation interchanges the left-handed and right-handed fields and conjugates the representations. The $SO(10)$ breaking with a Higgs 210-plet also yields the 422 symmetry, but the C -symmetry (and left-right (LR) symmetry) is explicitly broken in this case.

Previous investigations of particle spectroscopy in 422 models have relied on the presence of left-right symmetry [33], in order to keep the number of soft SUSY breaking parameters to a minimum. In this paper, we go a step further and assume that the soft scalar masses do not necessarily respect the discrete left-right symmetry. In principle, in the left-right asymmetric 422 model, the soft gaugino masses are not necessarily equal, $M_{SU(2)_L} \neq M_{SU(2)_R}$, and the SM hypercharge generator is given by

$$M_1 = \frac{3}{5}M_{2R} + \frac{2}{5}M_4, \quad (2.1)$$

where the $SU(4)$ gaugino mass parameter M_4 will be identified with M_3 . Then, if the 422 gaugino masses are independent, this will also hold for the SM gaugino masses. With additional assumptions, the number of free parameters can be reduced. Here, we will follow the approach of Ref. [26, 33] for the gaugino sector. Supplementing 422 with a discrete left-right C -symmetry, reduces the number of independent gaugino masses from three to two. Indeed, while the gaugino masses associated with $SU(2)_L$ and $SU(2)_R$ are the same, the gluino mass, associated with $SU(4)_c$, in principle can be different. The hypercharge generator from 422 implies:

$$M_1 = \frac{3}{5}M_2 + \frac{2}{5}M_3. \quad (2.2)$$

Our framework is the following: we assume that SUSY breaking occurs in a hidden sector at a scale $M_X > M_{GUT}$, via a mechanism that generates flavour-blind soft terms

in our visible sector. Between the scales M_X and M_{GUT} , while the theory still preserves the 422 symmetry, renormalisation and additional flavour symmetries may induce non-universalities for soft terms that belong to different representations (while particles that belong to the same representation have common soft masses).

We employ GUT relations among the soft terms derived from the unification group structure [36–41]. The soft terms for the scalar fields in an irreducible representation r of the 422 unification group are defined as multiples of a common scale m_0 :

$$m_r = x_r m_0, \quad (2.3)$$

while the trilinear terms are defined as

$$A_r = Y_r A_0, \quad A_0 = a_0 m_0. \quad (2.4)$$

Here, Y_r is the Yukawa coupling associated with the r representation and a_0 is a dimensionless factor, which is representation independent (the representation dependence is taken into account in the Yukawa couplings).

In view of the above discussion, we expect the following:

- Gluino masses: We assume the relation in eq. (2.2) among gaugino masses. We will see that this relation will yield gluino coannihilation as a viable scenario [34, 35], which was absent in other groups, namely SO(10), SU(5) and flipped SU(5) [36].
- Soft masses: Sfermions are accommodated in 16-dimensional spinor representations and their soft mass parameter is m_{16} . The electroweak MSSM doublets lie in the 10-dimensional representation with D-term contributions that result in splitting of their soft masses. Indeed, $m_{H_{u,d}}^2 = m_{10}^2 \pm 2M_D^2$, and, in our notation:

$$x_u = \frac{m_{H_u}}{m_{16}}, \quad x_d = \frac{m_{H_d}}{m_{16}}, \quad (2.5)$$

with $x_u < x_d$.

- LR asymmetric 422: In this case there is additional freedom, as the left-right asymmetry introduces a new parameter

$$x_{LR} = \frac{m_L}{m_R}, \quad (2.6)$$

where m_L is the mass of the left-handed sfermions (that preserve the definition of $m_{16} = m_0$), and m_R the mass of the corresponding right-handed ones.

3 Exploring the model: Methodology

We perform parameter space scans similar to [36], where the initial conditions of the soft terms are determined by a unification group that breaks at M_{GUT} (defined as the scale where the g_1 and g_2 couplings meet, while $g_3(M_{GUT})$ is obtained by requiring $\alpha_s(M_Z) =$

0.187). For our analysis we use Superbayes [42–44], a package to perform statistical inference of SUSY models which is linked to SoftSusy [45] to compute the SUSY spectrum, to MicrOMEGAs [46] and DarkSUSY [47] to compute DM observables, SuperIso [48] to compute flavour physics and the muon $g - 2$, and it uses Multinest [49] for sampling the parameter space of the models.

The likelihood function, which drives our exploration of regions of the parameter space where the model predictions fit the data well, is built from the following components:

$$\begin{aligned} \ln \mathcal{L}_{\text{Joint}} = & \ln \mathcal{L}_{\text{EW}} + \ln \mathcal{L}_{\text{B(D)}} + \ln \mathcal{L}_{\Omega_\chi h^2} \\ & + \ln \mathcal{L}_{\text{DD}} + \ln \mathcal{L}_{\text{Higgs}} + \ln \mathcal{L}_{\text{SUSY}} + \ln \mathcal{L}_{g-2}. \end{aligned} \quad (3.1)$$

Here:

- \mathcal{L}_{EW} is the part corresponding to electroweak precision observables, where constraints from LEP and Tevatron are implemented as summarised in [50, 51].
- \mathcal{L}_{B} stands for B-physics constraints, from $BR(\bar{B} \rightarrow X_s \gamma)$, $R_{\Delta M_{B_s}}$, $\frac{BR(B_u \rightarrow \tau \nu)}{BR(B_u \rightarrow \tau \nu)_{SM}}$, $BR(\bar{B}_s \rightarrow \mu^+ \mu^-)$ and $BR(\bar{B}_d \rightarrow \mu^+ \mu^-)$, assuming Gaussian likelihoods [52]. For $BR(\bar{B}_s \rightarrow \mu^+ \mu^-)$ and $BR(\bar{B}_d \rightarrow \mu^+ \mu^-)$ we quote the total uncertainties found by adding in quadrature the theoretical [53] and experimental [54, 55] uncertainties.
- $\mathcal{L}_{\Omega_\chi h^2}$ is for measurements of the cosmological DM relic density. Assuming that the lightest neutralino is the dominant DM component, we include constraints from Planck temperature and lensing data $\Omega_\chi h^2 = 0.1186 \pm 0.0031$ [6], with a (fixed) theoretical uncertainty $\tau = 0.012$, following Refs. [43, 56, 57], to account for numerical uncertainties.
- \mathcal{L}_{DD} is for constraints from direct DM detection searches; we apply data from the Xenon-1T [14] and PICO-60 [16] experiments. The likelihood is computed with the DDCalc code [58], and for the computation of the spin-independent and spin-dependent neutralino-nucleon cross-sections, we adopt hadronic matrix elements determined by lattice QCD [59, 60].
- $\mathcal{L}_{\text{Higgs}}$ implements bounds obtained from Higgs searches at LEP, Tevatron and LHC via HiggsBounds [61] and LHC Higgs-boson bounds [1, 2]. For this we use HiggsSignals [62], assuming a 2 GeV theoretical uncertainty in the lightest Higgs mass computation.
- $\mathcal{L}_{\text{SUSY}}$ stands for sparticle searches at colliders. The constraints from SUSY searches at LEP and Tevatron are evaluated following the prescription proposed in [63].
- \mathcal{L}_{g-2} : We use the value $\delta a_\mu^{\text{SUSY}} = (28.7 \pm 8.2) \times 10^{-9}$ [30], which corresponds to a 3.6σ discrepancy with the SM prediction and relies on e^+e^- data.

The MultiNest [49] algorithm is used to scan the parameter space and identify regions compatible with the data, though we do not perform any statistical interpretation of the results. Instead, we select only model points that predict the value of all observables

within the 2σ interval (with σ obtained by summing in quadrature the experimental and theoretical errors); however, we go to 3σ for muon $g-2$. We combine the samples produced using logarithmic and linear priors of the model parameters. We finally produce scatter plots showing the correlations of pairs of parameters and/or observables in various planes.

4 Results of the parameter space scan

As mentioned above, we perform two scans: one with logarithmic priors that scan over a wide range of parameters as shown in Eq. 4.1 and another one with flat priors, that are appropriate for looking for correlations. In the first case, we find many points with Higgsino DM and resonances in the annihilation channels, while flat priors are more appropriate when searching for coannihilations.

The 422 non universal soft masses are parametrized using the following definitions:

$$\begin{aligned}
100\text{GeV} &\leq m_0 = m_L &&\leq 10\text{TeV} \\
-3000\text{GeV} &\leq M_3 &&\leq 5\text{TeV} \\
50\text{GeV} &\leq M_2 &&\leq 5\text{TeV} \\
-10\text{TeV} &\leq A_0 &&\leq 10\text{TeV} \\
2 &\leq \tan\beta &&\leq 65 \\
-1 &\leq x_u &&\leq 2 \\
0 &\leq x_d &&\leq 3 \\
-3 &\leq x_{LR} = m_R/m_L &&\leq 3.
\end{aligned}
\tag{4.1}$$

Here M_1 is determined by eq. (2.2). Note that M_3 and m_R are allowed to be negative.

It is well known that if the required amount of relic DM is provided by neutralinos, particular mass relations must be present in the supersymmetric spectrum [64–71]. We therefore use these mass relations, together with the neutralino composition, in order to classify the points that pass the constraints discussed in Sec. 2, according to the following criteria:

Higgsino χ_1^0 :

$$h_f > 0.1, \quad |m_A - 2m_\chi| > 0.1 m_\chi. \tag{4.2}$$

The Higgsino-like fraction of the lightest neutralino mass eigenstate is characterized by the quantity

$$h_f \equiv |N_{13}|^2 + |N_{14}|^2, \tag{4.3}$$

where the N_{ij} are the elements of the unitary mixing matrix that correspond to the Higgsino mass states. In this case, the lightest chargino χ_1^\pm and the second lightest neutralino χ_2^0 are almost degenerate in mass with the χ_1^0 . The couplings to the SM gauge bosons are not suppressed and χ_1^0 pairs have large cross sections for annihilation into W^+W^- and ZZ pairs, which may reproduce the observed value of the relic abundance. Clearly, coannihilation channels involving χ_1^\pm and χ_2^0 also contribute.

A/H resonances:

$$|m_A - 2m_\chi| \leq 0.1 m_\chi. \quad (4.4)$$

The correct value of the relic abundance is achieved thanks to s -channel annihilation, enhanced by the resonant A propagator. The thermal average $\langle \sigma_{ann} v \rangle$ spreads out over the peak in the cross section, so that neutralino masses for which $2m_\chi \simeq m_A$ is not exactly realized can also experience resonant annihilations.

$\tilde{\tau}$ coannihilations:

$$h_f < 0.1, \quad (m_{\tilde{\tau}_1} - m_\chi) \leq 0.1 m_\chi. \quad (4.5)$$

The neutralino is bino-like, annihilations into leptons through t -channel slepton exchange are suppressed, and coannihilations involving the nearly-degenerate $\tilde{\tau}_1$ are necessary to enhance the thermal-averaged effective cross section.

$\tilde{\tau} - \tilde{\nu}_\tau$ coannihilations:

$$h_f < 0.1, \quad (m_{\tilde{\tau}_1} - m_\chi) \leq 0.1 m_\chi, \quad (m_{\tilde{\nu}_\tau} - m_\chi) \leq 0.1 m_\chi. \quad (4.6)$$

This is similar to the previous case but, in addition, the $\nu_{\tilde{\tau}}$ is nearly degenerate in mass with $\tilde{\tau}_1$.

\tilde{t}_1 coannihilations:

$$h_f < 0.1, \quad (m_{\tilde{t}_1} - m_\chi) \leq 0.1 m_\chi. \quad (4.7)$$

The \tilde{t}_1 is light and nearly degenerate with the bino-like neutralino. These coannihilations were found to be present also in the flipped SU(5) model, but not in SO(10) or SU(5) [36].

What is particularly interesting in the 422 model, which distinguishes it from the other GUT groups, is that in this case we get *three additional modes of coannihilation*, namely:

- **$\tilde{\chi}^+$ coannihilations:**

$$h_f < 0.1, \quad (m_{\tilde{\chi}^+} - m_\chi) \leq 0.1 m_\chi. \quad (4.8)$$

The lightest chargino is light and nearly degenerate with the bino-like neutralino.

- **\tilde{g} coannihilations:**

$$h_f < 0.1, \quad (m_{\tilde{g}} - m_\chi) \leq 0.1 m_\chi, \quad (4.9)$$

since the gluino can be relatively light and nearly degenerate with the bino-like neutralino.

- **\tilde{b} coannihilations:**

$$h_f < 0.1, \quad (m_{\tilde{b}} - m_\chi) \leq 0.1 m_\chi, \quad (4.10)$$

since, due to the LR asymmetry, the \tilde{b} can be light and nearly degenerate with the bino-like neutralino [72].

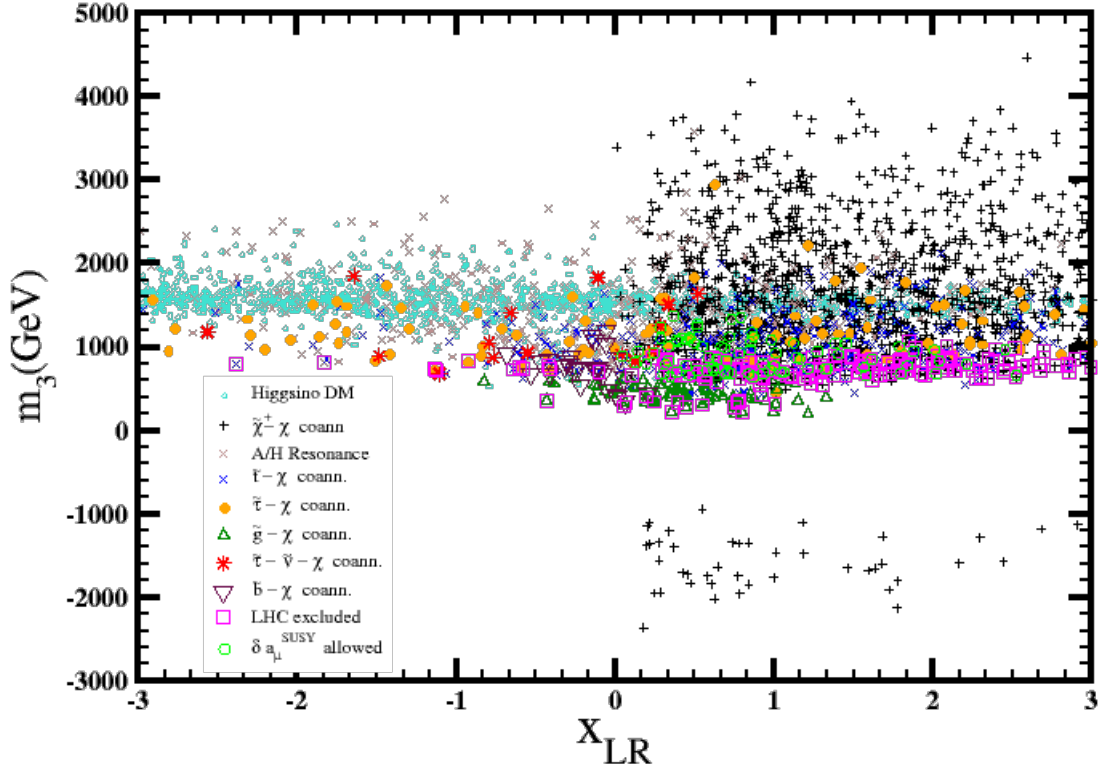


Figure 1. Correlation of the WMAP allowed points with the GUT values of M_3 and the LR sfermion mass ratio. Different kinds of points are denoted with a symbol and color code that also will be maintained in the rest of the plots: Turquoise dots correspond to Higgsino DM, black crosses to $\tilde{\chi}^\pm - \chi$ coannihilations, brown crosses to A/H resonances, blue crosses to $\tilde{\tau} - \chi$ coannihilations, orange dots to $\tilde{\tau} - \chi$ coannihilations, green up triangles to $\tilde{g} - \chi$ coannihilations, red stars to $\tilde{\tau} - \tilde{\nu} - \chi$, and maroon down triangles to $\tilde{b} - \chi$ coannihilations. In addition, green circles enclose points that provide a SUSY contribution to $\delta a_\mu^{\text{SUSY}}$ compatible with the experimental bounds, while points enclosed in magenta squares are excluded in our analysis of LHC results (see Sec. 5).

4.1 GUT inputs and Planck compatible regions

In this subsection we present the phenomenological consequences of relaxing the universality of the SUSY breaking terms following the 422 pattern. Specifically, we concentrate on the differences with respect to the groups based on SO(10) and SU(5) that assume gaugino mass universality. As discussed in Sec. 2, following the 422 group structure, the gaugino masses are not universal at the GUT scale, and we also assume left-right asymmetry for the scalar soft masses at the GUT scale. In the figures that follow, we show combined points arising from the linear and logarithmic sampling of parameters. In both cases, $\tilde{\chi}^+$ coannihilations and Higgsino DM are the points found most frequently.

In **Figure 1** we clearly observe that the vast majority of points lie in the upper right region. Points with $\tilde{\chi}^+$ coannihilations have a preference for $x_{LR} > 0$. We find that obtaining the correct prediction of m_h imposes a correlation between the signs of M_3 and A_0 . The majority of models satisfying this constraint correspond to $M_3 > 0$ and $A_0 < 0$, however, a few models with $M_3 < 0$ and $A_0 < 0$ are also found.

We observe that most of the classes of models satisfying the Planck constraints can be found even if sfermion LR symmetry is preserved. However, points with $\tilde{\tau} - \tilde{\nu}_\tau - \chi$ (red asterisks) and $\tilde{b} - \chi$ (maroon down triangles) coannihilations appear only when the LR symmetry is broken ($x_{LR} < 1$). Although the constraints imposed by the anomalous magnetic moment of the muon and the LHC searches will be discussed in the following sections, we find it illustrative to anticipate our results in all the plots. Therefore, we enclose in a green circle the points that explain the discrepancy of the experimental bound with respect to the SM prediction at the $3 - \sigma$ level. Similarly, points excluded by the LHC searches, according to the analysis presented in Sec. 5, are enclosed in magenta squares.

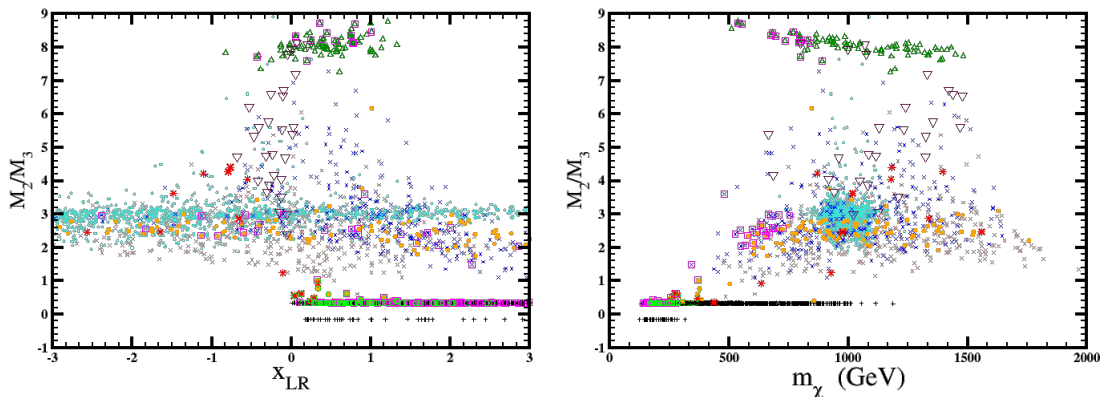


Figure 2. Scatter plots showing the different Planck areas as functions of the ratios of the GUT values for the soft terms, using the same notation as in Figure 1

The consequences of relaxing the gaugino mass universality can be appreciated in the left panel of **Figure 2**, where we can see how eq. (2.2) results in narrow ranges of M_2/M_3 for which m_χ approaches $m_{\tilde{\chi}^+}$; this gives rise to $\tilde{\chi}^+ - \chi$ coannihilations, almost independently of the neutralino mass and the LR ratio x_{LR} . These coannihilations are associated with ratios $M_2/M_3 \sim 0.4$ if $M_3 > 0$, and $M_2/M_3 \sim 0.2$ if $M_3 < 0$. In both cases, the lightest chargino is mostly wino and $x_{LR} > 0$. We also find points with $\tilde{\chi}^+ - \chi$ coannihilations for different values of M_2/M_3 , for cases where $\tilde{\chi}^+$ is not a pure wino. Coannihilations $\tilde{\tau} - \tilde{\nu} - \chi$ where the $\tilde{\tau}$ is mostly left-handed, correspond to $|x_{LR}| < 1$, while larger values of $|x_{LR}|$ allow right handed stau dominated $\tilde{\tau} - \chi$, as well as $\tilde{t} - \chi$ coannihilations. In order to classify coannihilations of the LSP with a sparticle \tilde{p} , we used as a criterion a mass ratio $m_{\tilde{p}}/m_\chi = 0.1$, although we can see that coannihilations among several particles are also possible. Some coannihilation points classified as $\tilde{\tau} - \chi$ and $\tilde{\tau} - \tilde{\nu} - \chi$ show ratios M_2/M_3 typical of the chargino coannihilations, indicating that coannihilations $\tilde{\tau} - \tilde{\nu} - \tilde{\chi}^+ - \chi$ are possible. The neutralino masses satisfying the Planck constraints are displayed in the right panel of **Figure 2**. We can see that points satisfying the muon ($g - 2$) constraints require values of m_χ below 500 GeV, and all of them correspond to ratios M_2/M_3 below 2. Higgsino like neutralino masses are in the 1 TeV range, similar to what was found in other

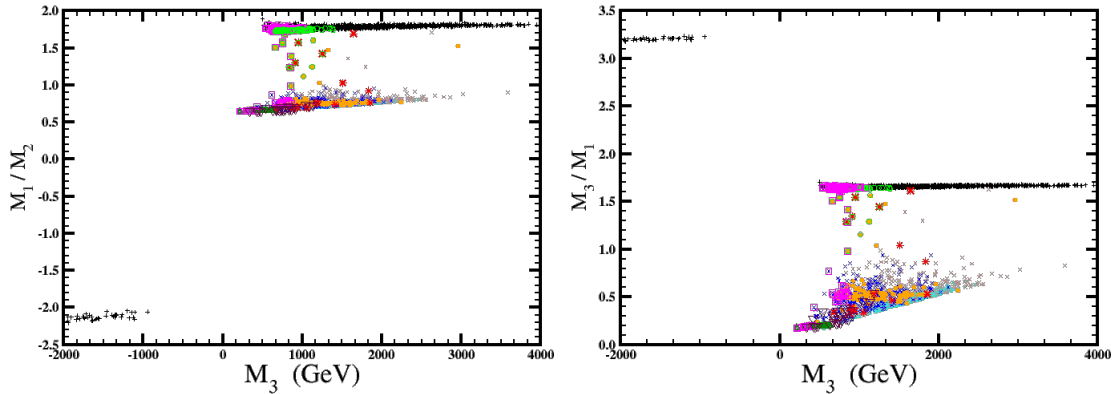


Figure 3. Values of the gaugino mass ratios vs M_3 at the GUT scale and their correlation with the different Planck areas as functions of the GUT ratios for the soft terms. We use the same notation as in Figure 1.

GUTs [36]. We can see again that LR asymmetry allows $\tilde{\tau} - \tilde{\nu} - \chi$ and $\tilde{b} - \chi$ coannihilations that are not present when the LR symmetry holds ($x_{LR} = 1$).

Figure 3 provides a clear picture of the constraints imposed by gaugino mass relations, as shown in eq. (2.2), along with the Planck constraints. These may imply a second condition on the gaugino masses due to relations of the LSP mass with other particles in order to fulfill the relic density requirements; this relation is more diffuse, due to RGE dependence at the low energy mass scale. In the left panel, we can see that two ratios are favored: $M_1/M_2 \sim 1.8$ and $M_1/M_2 \sim -2.1$ (the latter corresponds to $M_3 < 0$). Due to eq. (2.2), these regions can be correlated to $M_3/M_1 \sim 2.2$ and $M_3/M_1 \sim 3.2$, respectively, in the right panel. Moreover, $\tilde{g} - \chi$ coannihilations are produced by ratios of $M_3/M_1 \sim 0.2$ that correspond to ratios of $M_1/M_2 \sim 0.53$. Points with Higgsino DM and A/H resonances appear for narrow ranges of the ratio M_3/M_1 . This is due to the fact that they impose additional constraints on the gaugino masses, decreasing the μ -term so that the Higgsino component of the LSP becomes relevant and/or the A/H resonance condition $m_\chi/2 \sim m_{A/H}$ is materialised. In both cases, the approximate range 0.3-0.5 for M_3/M_1 is converted by Eq. (2.2) to a range 0.6-0.9 for M_1/M_2 . A very distinct case arises for $\tilde{\chi}^+ - \chi$ coannihilations, in the case where the neutralino and the chargino are almost bino- and wino-like respectively. For sfermion coannihilations, the relations among the GUT values of the gaugino masses are not as sharp. Stop coannihilations, due to the effect of the stop mass in the RGE's, depend on the value of M_3/M_1 and, through eq. (2.2), on M_1/M_2 as well. Stau coannihilations, however, are not affected by M_3/M_1 and can take values between the limiting lines characteristic of Higgsino DM and chargino coannihilation.

4.2 Higgs mass and Muon ($g - 2$)

Connecting the Higgs boson discovery with the lightest neutral SUSY particle of the MSSM requires a rather heavy SUSY spectrum that makes it challenging to explain the discrepancy between the experimental value of $(g_\mu - 2)$ and its SM prediction, at least in the simplest SUSY models. The value $\delta\alpha_\mu^{SUSY} = (28.7 \pm 8.2)10^{-10}$ is difficult to reach in models with universal soft terms. Even after allowing non-universalities at the GUT scale for scalar soft terms, like the models based on SU(5) and SO(10) of Ref. [36], the SUSY contribution

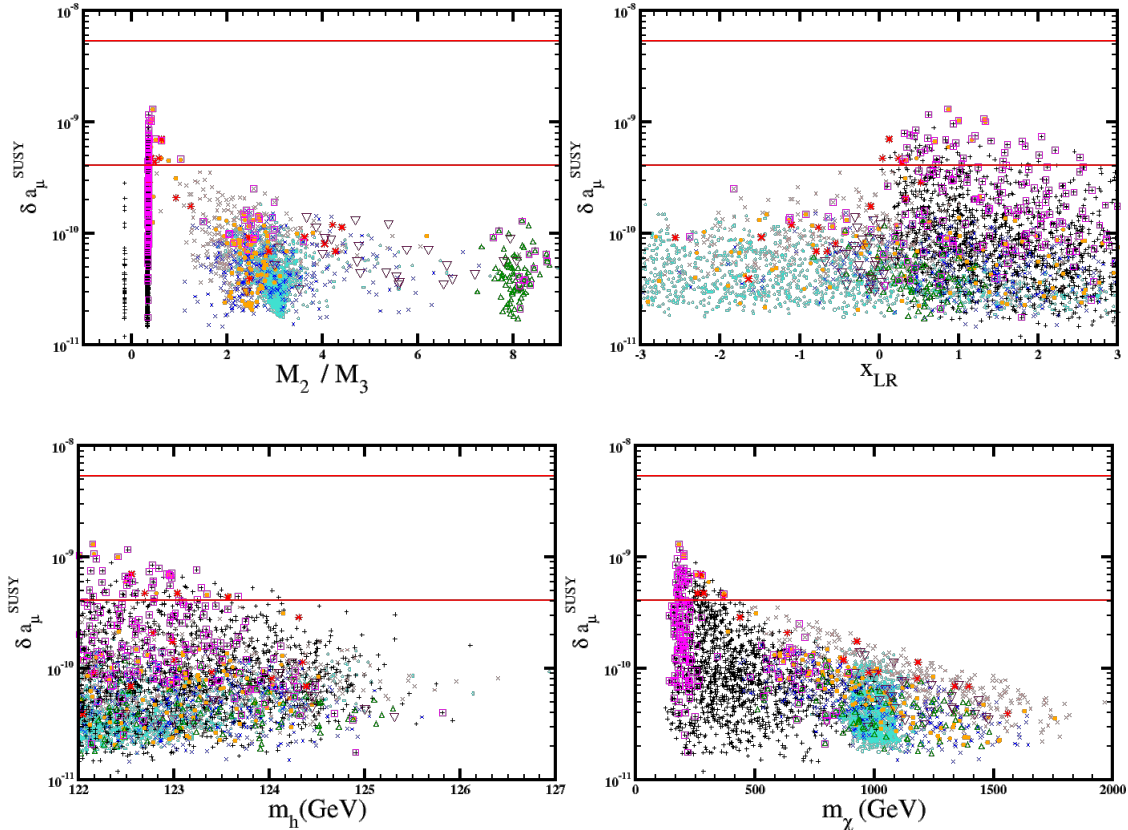


Figure 4. The upper panels show the variation of the prediction for δa_μ^{SUSY} with the ratio of the GUT values of M_2/M_3 (left) and the LR asymmetry of the GUT values for the sfermion masses (right). The lower panels show regions satisfying δa_μ^{SUSY} and m_h bounds (left) and δa_μ^{SUSY} vs m_χ (right). The red lines are the $3\text{-}\sigma$ bound lines for the experimental discrepancy of a_μ with respect to the SM prediction.

remains below the central value. Therefore, we wish to investigate whether the pattern of soft terms introduced by the 422 symmetry can result in models with a larger contribution to muon ($g - 2$).

To display the relevance of the particular relation of soft terms introduced by the 422 symmetry, we present in the upper panels of **Figure 4** the variation of the prediction of δa_μ^{SUSY} with the GUT gaugino mass ratios (left) and the LR asymmetry (right). We can observe that the highest values of δa_μ^{SUSY} are obtained for M_2/M_3 ratios that favor chargino coannihilations. We also see that only M_2/M_3 below 2 can result in a SUSY contribution compatible with $(g_\mu - 2)$. The right upper panel shows that the LR soft mass asymmetry results in some points with $\tilde{\tau} - \chi$ coannihilations crossing the δa_μ^{SUSY} lower bound. These points include cases where the stau is mostly left-handed, so that $\tilde{\tau} - \tilde{\nu} - \chi$ coannihilations take place.

In the lower panels of **Figure 4**, we explore the m_χ values that can simultaneously explain the experimental value of the Higgs mass and the discrepancy δa_μ . A SUSY contribution to δa_μ^{SUSY} above the lower bound is possible for points with chargino and stau-coannihilations for $m_\chi < 500$ GeV. Note that many of the points of [73, 74] satisfying

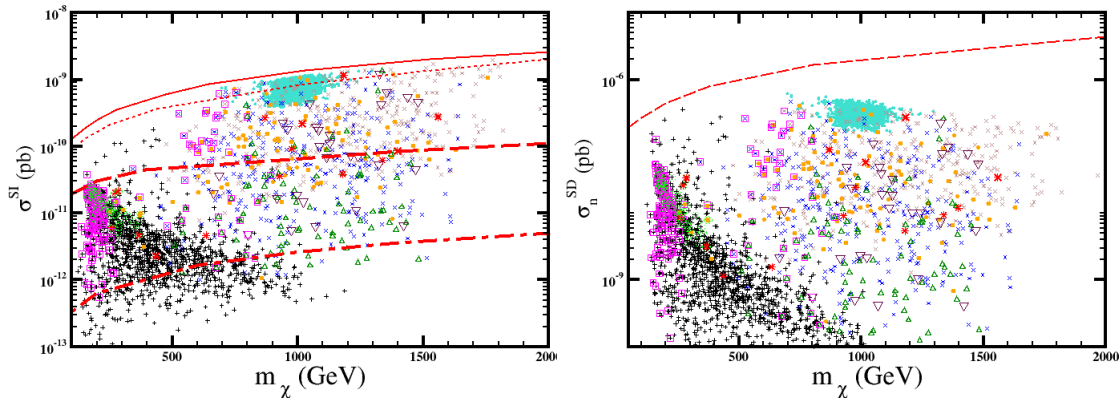


Figure 5. *Left panel: scatter plot for the SI neutralino-nucleon cross section; the upper red line corresponds to the Xenon-1T bound [14] and the dotted line below, to its recent update [75]. The dash and the dot-dash lines correspond to the projected sensitivities from LZ[12] and DARWIN [15]. Right panel: same plot for the SD neutralino-neutron cross section and the projected limit from LZ [12].*

δa_μ^{SUSY} are now excluded because of the m_h bound (and will be further constrained by the LHC, as we will discuss in section 5).

4.3 Dark Matter Searches

The current choice of soft terms allows for models where the neutralino relic density is located inside the cosmological bounds in scenarios that imply different relations among SUSY masses. In each scenario, the composition of the LSP determines its detection prospects.

In **Figure 5** we display the Spin Independent (SI) and Spin Dependent (SD) neutralino-nucleon cross sections as functions of the neutralino mass, comparing the theoretical predictions with updated experimental bounds, as summarised in the respective figure captions (the line corresponding to the latest announced update from Xenon-1T [75] is also included). The SI bounds are the most restrictive, and the current bounds from Xenon-1T [14] exclude many models where the LSP has a relevant Higgsino component. According to our classification of section 4, these correspond to Higgsino DM ($h_f > 0.1$). However, points where the LSP has a smaller Higgsino component, such as A/H resonances, are on the scope of coming experiments like LZ [12]. Furthermore, even models where the LSP has a high degree of bino purity can be reached at sensitivities such as the ones expected with a multi-ton mass experiment like the DARWIN project [15]. These experiments can explore most of the models presented here, including the $(g_\mu - 2)$ favored points.

Regarding the SD neutralino-nucleon cross section, bounds from experiments sensitive to neutralino-proton interactions like PICO[16] are less restrictive than the SI case. Models predicting SI cross sections on the Xenon-1T bound are below the PICO bound by two orders of magnitude. The predictions for neutralino-neutron cross sections, like the ones displayed in the right panel of **Figure 5** are higher. However, we can see on the figure that the LZ prospects still favors the SI over the SD interaction sensitivity.

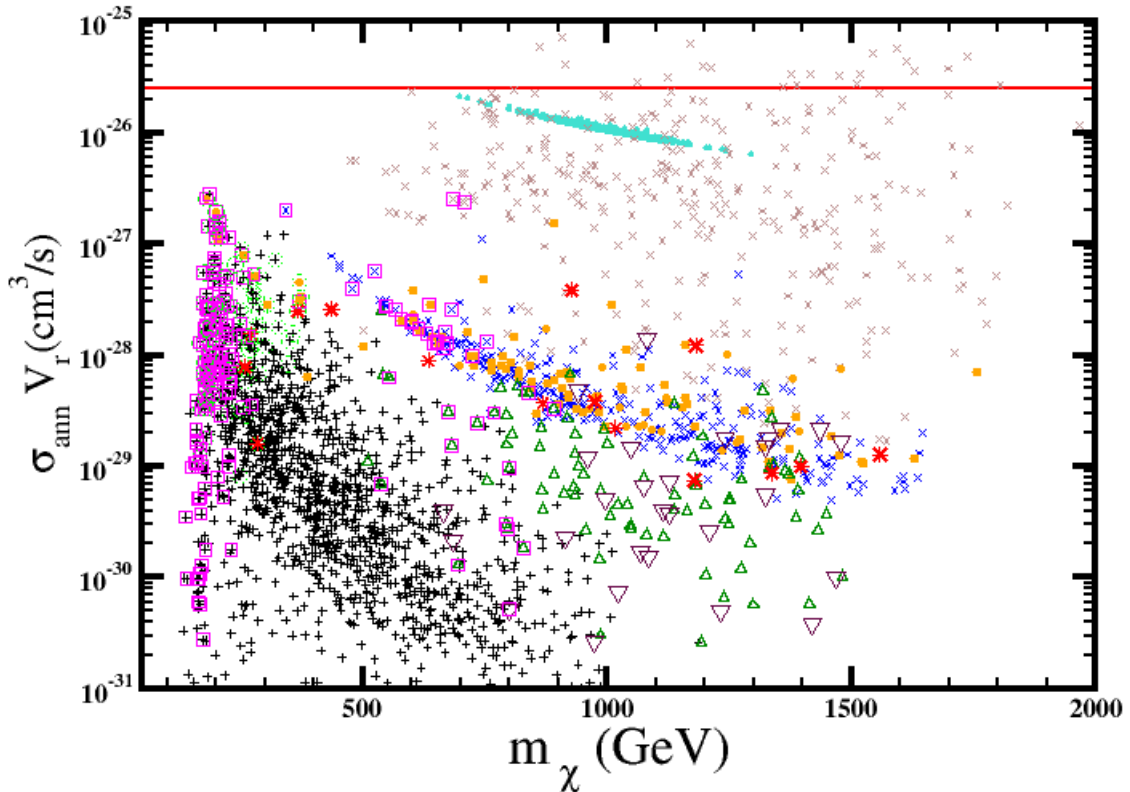


Figure 6. Scatter plot for the total non-relativistic LSP annihilation cross section times relative velocity as a function of the neutralino mass. The red line corresponds to the usual benchmark value of $\langle \sigma_{\text{eff}} v_{\text{rel}} \rangle \simeq 2 - 3 \times 10^{-26} \text{ cm}^3/\text{s}$.

Figure 6 depicts the total non-relativistic LSP annihilation cross section times relative velocity as a function of the neutralino mass. Here as well, we see that for a subset of points like Higgsino DM and A/H resonances where the neutralino has an important Higgsino component and we hope that further light can be shed in the near future.

5 LHC searches

In previous sections we have seen how the implementation of the 422 group expands the possibilities for DM predictions with respect to more constrained models. In this section, we derive sparticle mass correlations, combining the experimental and cosmological data summarised in the previous sections with results from applying the LHC constraints. The results indicate the complementarity of DM experiments and of LHC SUSY searches for the asymmetric 422 group, similar to what was found in other GUTs [36].

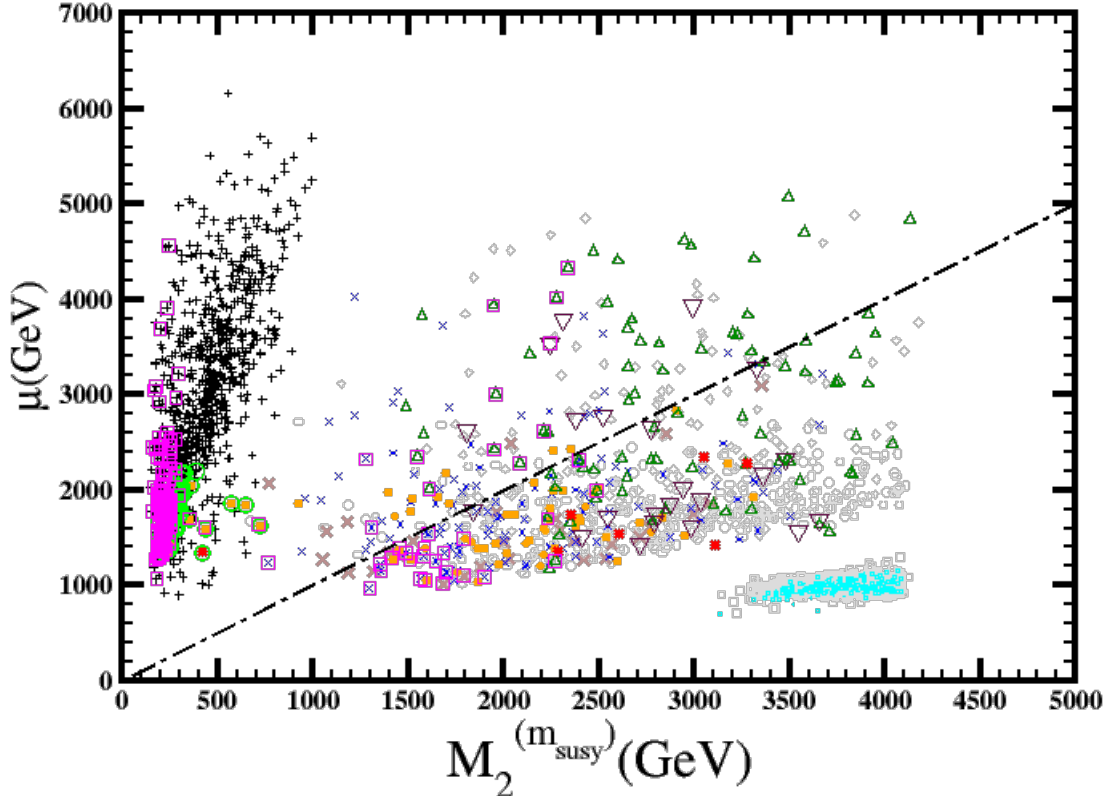


Figure 7. Scatter plots in the $\mu - M_2$ plane. Only points analyzed with *Smodels* are shown with the same legends as in previous figures (the brown crosses corresponding to A/H resonances are thicker than in the previous plots). The gray symbols correspond to points not analyzed with *Smodels*, squares are for Higgsino DM, circles for A/H resonances and diamonds for stop coannihilations. The dot-dash line represents $\mu = M_2$.

The so far unsuccessful searches for SUSY particles impose severe bounds on their spectrum and interactions. However, it is not straightforward to translate these bounds to SUSY masses, because the ATLAS and CMS experiments typically show results in a model-dependent fashion. Namely, the recast of the data is done in the framework of so-called Simplified Model Spectra (SMS) that can be considered indicative rather than conclusive for real models [77, 78].

Every SMS can be defined by a set of hypothetical particles and a sequence of their products and decay modes. Therefore, to confront the theoretical models against the LHC bounds, the predictions must be expressed in the SMS language. There are several tools designed for such purpose [79–81] and by using these packages, we can go one step further in comparing our models with LHC data, applying this procedure to a large number of models without the need of a huge computing power [82, 83].

In our analysis, we compute for every model its particle mass spectrum using *SoftSusy* [45] and the decay branching ratios (\mathcal{B}) using *SUSY-HIT* [86]. Then, we pass this information to *Smodels-v1.1.1*. [79] in form of a SLHA [84] file. Production cross-sections (σ) are calculated by *Smodels-v1.1.1* which calls *Pythia 8.2* [85].

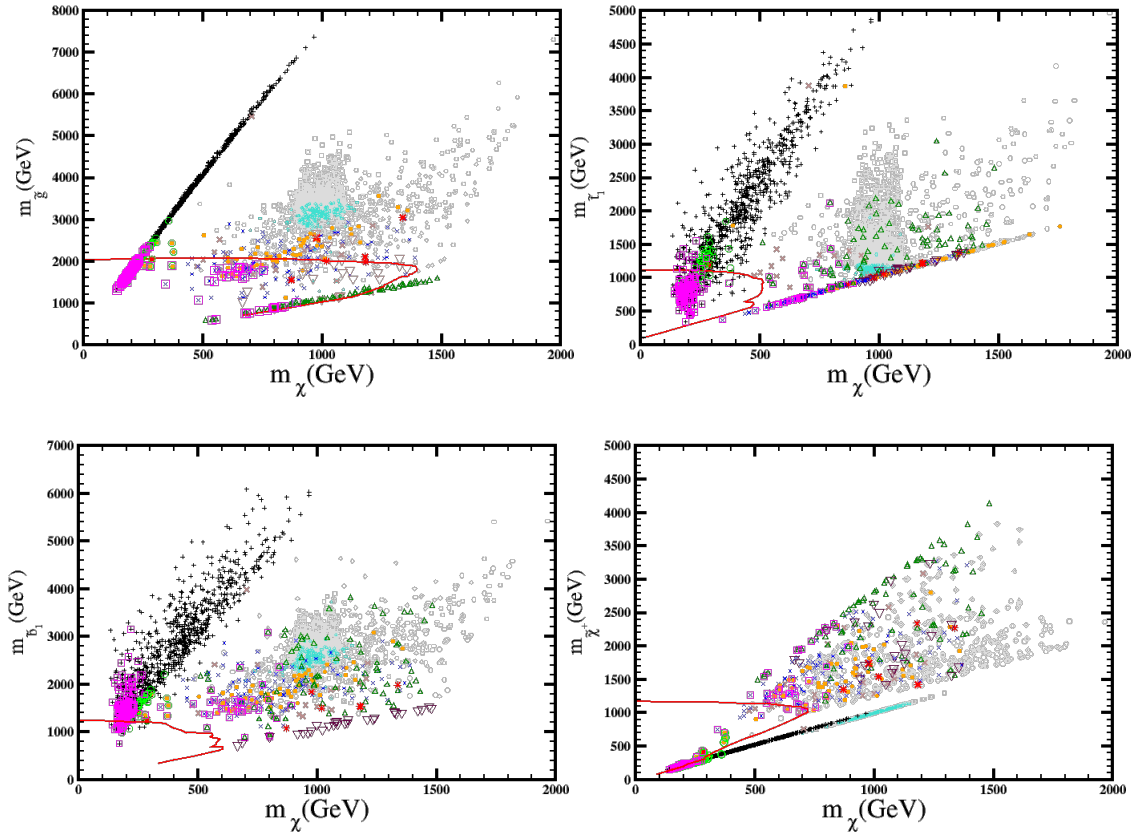


Figure 8. The impact of the LHC searches on the 422 models from diverse bounds obtained by ATLAS and CMS. For the points we use the same code as in Figure 1. The solid red line corresponds to the CMS bound applied to simplified SUSY scenarios while the points in the purple squares are excluded by the same bounds applied to the predictions of our models using Smodels.

Smodels-v1.1.1 decomposes production chains in SMS topologies that are confronted with the ones constrained by data. It cannot test all the models we provide, either because their topologies do not match any of the existing experimental results or because their masses fall outside the ranges considered by the experimental searches. These models along with models with weak signals (below 0.05 fb) are considered as beyond the scope of the LHC and classified as not tested. Besides if the mass gap between mother and daughter is small, the decays products will be too soft to trigger any signal. We use 5 GeV as the minimum required mass difference for the decay products to be visible.

In order to present our results, we distinguish among models where the SMS results apply ¹ and the ones not tested ². For the first, we keep the notation from the previous sections, while not tested models are displayed as gray symbols (squares for Higgsino DM, circles for A/H resonances, diamonds for the \tilde{t} -coannihilation). Not tested models are about 50% of the total investigated models; however this percentage changes depending on the class of models. For clarity reasons we display only the cases where the number of not-tested models dominates over the analysed ones (Higgsino DM, A/H resonances and

¹SMS results that test the specific topology exist.

²When no simplified model result exists for the signal topologies of the point considered.

\tilde{t} -coannihilation). The other classes of models lie in the same areas of the graphs as the displayed points.

In Figure 7, we display μ versus M_2 at $m_{susy} = \sqrt{m_{\tilde{t}_1} m_{\tilde{t}_2}}$ in order to infer the composition of the lightest chargino. We can see that the models with gaugino-dominant charginos are classified as $\tilde{\chi}^\pm - \chi$ coannihilations; we also notice that up to a value of $M_2(m_{susy}) \sim 300$ GeV, many of these models are affected by the LHC exclusion bounds.

In Figure 8 we show the impact of LHC constraints in some of the mass planes. The results can be summarized as follows:

- On the top left panel we show the impact of strong production through the 0-lepton + jets + \cancel{E}_T channel where the excluded points can be compared with the current coverage by CMS [88, 89] using SMS results. It is interesting to notice that there are points with gluino masses about 1.3 TeV away from the gluino-compress region, for which the 13 TeV searches should have good sensitivity, which are not excluded by the SMS results. The reason for this is that the produced gluino-pairs decay asymmetrically via, for instance, one into $b\bar{b}$ and the another one into light jets. It is also visible how there are points in the gluino-compress spectra region sensitive to monojet searches. Besides, due to the correlations of the gaugino masses induced by GUT-scale boundary conditions imposed by the model some of the points lying into the chargino-coannihilations region are also excluded by this search. These conclusion hold for the exclusion of squarks.
- Next we show the impact of the third generation squarks searches on both stop/sbottom-neutralino mass planes on top right panel and bottom left panel respectively. For stops a reasonable correspondence is found between the sensitivity to the model points and those of the simplified-model decay considered in ATLAS and CMS analyses [90–93], in which the top squark was assumed to decay to $t + \chi^\pm$. Beyond these points, points not excluded typically undergo long chain decays. For the sbottoms the impact of the LHC constraints is rather weak since for light neutralinos, sbottoms are too heavy to be excluded. Points with sensitivity are well captured by a simplified model where the sbottom decays into a bottom quark and a neutralino.
- Finally, the impact of electroweak searches through the multi-leptons + \cancel{E}_T channel [94] is shown in the chargino-neutralino mass plane in the bottom right panel. The largest impact of this channel is on the chargino-coannihilation region through the soft two-lepton channel which is sensitive to compress spectrum, specially for wino-like charginos. As it can be seen, most of the points with $m_{\tilde{\chi}^\pm} \lesssim 300$ GeV are excluded by this search. As it is mentioned this search is complementary to the 0-lepton + jets + \cancel{E}_T search.

The impact of this search to sleptons is however insignificant because slepton production cross sections are small. The lower values for the slepton masses are of the order of 300 GeV for the staus and 400 GeV for the other generations.

In order to compare the 422 LHC predictions with other possible signals of the 422 modes, we can consider several reference values for the LSP masses and see the correspon-

dence among different plots. For instance, for values of m_χ below 500 GeV we find models that satisfy the muon (g -2) $3 - \sigma$ bound. These points (in green circles) are classified as models with $\tilde{\chi}_+$ or $\tilde{\tau}$ coannihilations. Since their mass spectrum is relatively low, many of them are excluded by the current LHC bounds according to *Smodels*. From future experiments, only the sensitivity of DARWIN will suffice to explore this area. Their indirect detection signals are also weak since they lie two orders of magnitude below the reference line of Figure 6.

The 422 structure for the soft terms allows coannihilations at values of $m_\chi \approx 1$ TeV and beyond, which is not possible in models with universal soft-terms like the CMSSM. The analysis with *Smodels* indicate that many of the classes of models produce signals that can be compared with the LHC bounds up to values of m_χ about 1.5 TeV. Beyond this mass we find only models with A/H resonances and \tilde{t} coannihilations that are not tested with *Smodels*. In contrast, the predictions of these models are the most promising for indirect detection (see **Figure 6**) and they will be tested at Xenon-nT and LZ, before the sensitivity of DARWIN is reached as we can see in **Figure 6**.

6 Conclusions

In this work we explored the predictions of supersymmetric $SU(4)_c \times SU(2)_L \times SU(2)_R$ (422) models for supersymmetric particle spectra, taking into account the constraints from LHC and cold dark matter searches. The gauge and symmetry breaking structure of these models leads to very distinct predictions, which deviate significantly from other models.

In particular, our results are the following:

- A variety of coannihilation scenarios compatible with LSP dark matter and the LHC have been identified. This clearly indicates that, despite the fact that no SUSY signal has been found so far, there is still a lot of ground to cover and several alternative possibilities to explore.
- The particular relations between the gaugino masses in 422 result in relatively light gluinos with gluino coannihilations, a feature that is very particular for these models and does not appear in other GUT schemes. Similarly, chargino coannihilations are also found in this case, and in fact, together with Higgsino DM, are the most frequently encountered scenarios.
- The fact that the soft supersymmetry breaking parameters at M_{GUT} can be non-universal, while compatible with the 422 symmetry, gives rise to additional possibilities and unique features compared to other GUTs, including stop (also found in flipped SU(5), but not SO(10) or SU(5)) and sbottom coannihilations.
- We find very concrete predictions for the gaugino mass ratios that favor scenarios such as chargino-neutralino coannihilations. For sfermion-neutralino coannihilations (and particularly staus where there is no dependence on M_3/M_1), the gaugino mass relations that lead to viable schemes are not as sharp.
- Overall, the LHC and dark matter searches complement each other in covering the available parameter space, and among others, accommodate solutions with prospects for

reducing the muon $g - 2$ discrepancy via a SUSY contribution. These solutions are mostly found in the stau-neutralino and chargino-neutralino coannihilation areas.

Acknowledgments

M.E.G. research was supported by the Spanish MINECO, under grants FPA2014-53631-C-2-P and FPA2017-86380-P. R. RdA is supported by the Ramón y Cajal program of the Spanish MICINN, the Elusives European ITN project (H2020-MSCA-ITN-2015//674896-ELUSIVES), the “SOM Sabor y origen de la Materia” (PROMETEOII/2014/050) and Centro de excelencia Severo Ochoa Program under grant SEV-2014-0398. Q.S. acknowledges support by the DOE grant No. DE-SC0013880. We also thank F. Márquez Saldaña for useful discussions.

References

- [1] G. Aad *et al.* [ATLAS Collaboration], Phys. Lett. B **716** (2012) 1 [arXiv:1207.7214 [hep-ex]].
- [2] S. Chatrchyan *et al.* [CMS Collaboration], Phys. Lett. B **716** (2012) 30 [arXiv:1207.7235 [hep-ex]].
- [3] E. Komatsu *et al.* [WMAP Collaboration], Astrophys. J. Suppl. **192** (2011) 18 [arXiv:1001.4538 [astro-ph.CO]].
- [4] C. L. Bennett *et al.* [WMAP Collaboration], Astrophys. J. Suppl. **208** (2013) 20 [arXiv:1212.5225 [astro-ph.CO]].
- [5] P. A. R. Ade *et al.* [Planck Collaboration], Astron. Astrophys. **571** (2014) A16 [arXiv:1303.5076 [astro-ph.CO]].
- [6] P. A. R. Ade *et al.* [Planck Collaboration], Astron. Astrophys. **594** (2016) A13 [arXiv:1502.01589 [astro-ph.CO]].
- [7] H. Goldberg, Phys. Rev. Lett. **50** (1983) 1419 Erratum: [Phys. Rev. Lett. **103** (2009) 099905].
- [8] J. R. Ellis, J. S. Hagelin, D. V. Nanopoulos, K. A. Olive and M. Srednicki, Nucl. Phys. B **238** (1984) 453.
- [9] For a compendium of CMS searches for supersymmetry, see <https://twiki.cern.ch/twiki/bin/view/CMSPublic/PhysicsResultsSUS>.
- [10] For a compendium of ATLAS searches for supersymmetry, see <https://twiki.cern.ch/twiki/bin/view/AtlasPublic/SupersymmetryPublicResults>.
- [11] D. S. Akerib *et al.* [LUX Collaboration], Phys. Rev. Lett. **118** (2017) no.2, 021303 [arXiv:1608.07648 [astro-ph.CO]].
- [12] D. S. Akerib *et al.* [LUX-ZEPLIN Collaboration], arXiv:1802.06039 [astro-ph.IM].
- [13] E. Aprile *et al.* [XENON Collaboration], JCAP **1604** (2016) no.04, 027 [arXiv:1512.07501 [physics.ins-det]].
- [14] E. Aprile *et al.* [XENON Collaboration], Phys. Rev. Lett. **119** (2017) no.18, 181301/ [arXiv:1705.06655 [astro-ph.CO]].

- [15] J. Aalbers *et al.* [DARWIN Collaboration], JCAP **1611** (2016) 017 [arXiv:1606.07001 [astro-ph.IM]].
- [16] C. Amole *et al.* [PICO Collaboration], Phys. Rev. Lett. **118** (2017) no.25, 251301 [arXiv:1702.07666 [astro-ph.CO]].
- [17] J. C. Costa *et al.*, Eur. Phys. J. C **78** (2018) no.2, 158 [arXiv:1711.00458 [hep-ph]].
- [18] E. Bagnaschi *et al.*, Eur. Phys. J. C **78** (2018) no.3, 256 [arXiv:1710.11091 [hep-ph]].
- [19] P. Athron *et al.* [GAMBIT Collaboration], Eur. Phys. J. C **77** (2017) no.12, 824 [arXiv:1705.07935 [hep-ph]].
- [20] P. Athron *et al.* [GAMBIT Collaboration], Eur. Phys. J. C **77** (2017) no.12, 879 [arXiv:1705.07917 [hep-ph]].
- [21] E. Bagnaschi *et al.*, Eur. Phys. J. C **77** (2017) no.2, 104 [arXiv:1610.10084 [hep-ph]].
- [22] A. Fowlie, K. Kowalska, L. Roszkowski, E. M. Sessolo and Y. L. S. Tsai, Phys. Rev. D **88** (2013) 055012 [arXiv:1306.1567 [hep-ph]].
- [23] M. van Beekveld, W. Beenakker, S. Caron, R. Peeters and R. Ruiz de Austri, Phys. Rev. D **96** (2017) no.3, 035015 [arXiv:1612.06333 [hep-ph]].
- [24] M. E. Cabrera, J. A. Casas, A. Delgado, S. Robles and R. Ruiz de Austri, JHEP **1608** (2016) 058 [arXiv:1604.02102 [hep-ph]].
- [25] J. C. Pati and A. Salam, Phys. Rev. D **10**, 275 (1974).
- [26] R.N. Mohapatra and J.C. Pati, Phys. Rev. D **11**, 566 (1975); G. Senjanovic and R.N. Mohapatra, Phys. Rev. D **12**, 1502 (1975); M. Magg, Q. Shafi and C. Wetterich, Phys. Lett. B **87**, 227 (1979);
- [27] G. Lazarides and Q. Shafi, Nucl. Phys. B **189**, 393 (1981); T. W. B. Kibble, G. Lazarides and Q. Shafi, Phys. Lett. B **113**, 237 (1982).
- [28] S. F. King and Q. Shafi, Phys. Lett. B **422**, 135 (1998).
- [29] Jeannerot *et al.* JHEP 0010(2000)012; hep-ph/ 0002151.
- [30] M. Davier, A. Hoecker, B. Malaescu and Z. Zhang, Eur. Phys. J. C **71** (2011) 1515 Erratum: [Eur. Phys. J. C **72** (2012) 1874] [arXiv:1010.4180 [hep-ph]].
- [31] T. W. B. Kibble, G. Lazarides and Q. Shafi, Phys. Rev. D **26**, 435 (1982).
- [32] G. Lazarides and Q. Shafi, Phys. Lett. B **159**, 261 (1985).]
- [33] I. Gogoladze, R. Khalid and Q. Shafi, Phys. Rev. D **79** (2009) 115004 [arXiv:0903.5204 [hep-ph]].
- [34] M. Adeel Ajaib, T. Li and Q. Shafi, Phys. Lett. B **705** (2011) 87 [arXiv:1107.2573 [hep-ph]].
- [35] S. Raza, Q. Shafi and C. S. n, Phys. Rev. D **92** (2015) no.5, 055010 [arXiv:1412.7672 [hep-ph]].
- [36] M. Cannoni, J. Ellis, M. E. Gómez, S. Lola and R. Ruiz de Austri, JCAP **1603** (2016) no.03, 041 [arXiv:1511.06205 [hep-ph]].
- [37] S. Dar, I. Gogoladze, Q. Shafi and C. S. Un, Phys. Rev. D **84** (2011) 085015 [arXiv:1105.5122 [hep-ph]].
- [38] N. Okada, S. Raza and Q. Shafi, Phys. Rev. D **90** (2014) no.1, 015020 [arXiv:1307.0461 [hep-ph]].

- [39] K. Kowalska, L. Roszkowski, E. M. Sessolo and A. J. Williams, JHEP **1506** (2015) 020 [arXiv:1503.08219 [hep-ph]].
- [40] K. Kowalska, L. Roszkowski, E. M. Sessolo and S. Trojanowski, JHEP **1404** (2014) 166 [arXiv:1402.1328 [hep-ph]].
- [41] J. Ellis, J. L. Evans, A. Mustafayev, N. Nagata and K. A. Olive, Eur. Phys. J. C **76** (2016) no.11, 592 [arXiv:1608.05370 [hep-ph]].
- [42] G. Bertone, D. G. Cerdeno, M. Fornasa, R. Ruiz de Austri, C. Strege and R. Trotta, JCAP **1201** (2012) 015 [arXiv:1107.1715 [hep-ph]].
- [43] C. Strege, G. Bertone, F. Feroz, M. Fornasa, R. Ruiz de Austri and R. Trotta, JCAP **1304** (2013) 013 [arXiv:1212.2636 [hep-ph]].
- [44] G. Bertone, F. Calore, S. Caron, R. R. de Austri, J. S. Kim, R. Trotta and C. Weniger, arXiv:1507.07008 [hep-ph].
- [45] B. C. Allanach, Comput. Phys. Commun. 143 (2002) 305 [hep-ph/0104145]; <http://projects.hepforge.org/softsusy/>
- [46] G. Belanger, F. Boudjema, A. Pukhov and A. Semenov, " Comput. Phys. Commun. 176 (2007) 367; <http://lapth.in2p3.fr/micromegas/>
- [47] P. Gondolo, J. Edsjo, P. Ullio, L. Bergstrom, M. Schelke and E. A. Baltz, JCAP 0407 (2004) 008; <http://www.darksusy.org/>
- [48] F. Mahmoudi, Comput.Phys.Comm. 178 (2008) 745 and Comput.Phys.Comm. 180 (2009) 1579
- [49] F. Feroz and M. P. Hobson, Mon. Not. Roy. Astron. Soc. **384** (2008) 449463; F. Feroz, M. P. Hobson and M. Bridges, "MultiNest: an efficient and robust Bayesian inference tool for cosmology and particle physics," Mon. Not. Roy. Astron. Soc. **398**, 1601 (2009) [0809.3437]; <http://www.ft.uam.es/>
- [50] S. Schael *et al.* [ALEPH and DELPHI and L3 and OPAL and SLD and LEP Electroweak Working Group and SLD Electroweak Group and SLD Heavy Flavour Group Collaborations], "Precision electroweak measurements on the Z resonance," Phys. Rept. **427**, 257 (2006) [hep-ex/0509008].
- [51] K. A. Olive *et al.* [Particle Data Group Collaboration], "Review of Particle Physics," Chin. Phys. C **38**, 090001 (2014).
- [52] C. Strege, G. Bertone, G. J. Besjes, S. Caron, R. Ruiz de Austri, A. Strubig and R. Trotta, JHEP **1409** (2014) 081 [arXiv:1405.0622 [hep-ph]].
- [53] A. Arbey, M. Battaglia, F. Mahmoudi and D. Martinez Santos, Phys. Rev. D **87** (2013) no.3, 035026 [arXiv:1212.4887 [hep-ph]].
- [54] V. Khachatryan *et al.* [CMS and LHCb Collaborations], "Combination of results on the rare decays $B_{(s)}^0 \rightarrow \mu^+ \mu^-$ from the CMS and LHCb experiments," CMS-PAS-BPH-13-007, LHCb-CONF-2013-012, CERN-LHCb-CONF-2013-012;
- [55] V. Khachatryan *et al.* [CMS and LHCb Collaborations], Nature **522** (2015) 68 [arXiv:1411.4413 [hep-ex]].

- [56] L. Roszkowski, R. Ruiz de Austri, R. Trotta, Y. L. S. Tsai and T. A. Varley, Phys. Rev. D **83** (2011) no.1, 015014 Erratum: [Phys. Rev. D **83** (2011) no.3, 039901] [arXiv:0903.1279 [hep-ph]].
- [57] L. Roszkowski, E. M. Sessolo and A. J. Williams, JHEP **1408** (2014) 067 [arXiv:1405.4289 [hep-ph]].
- [58] C. Savage, A. Scaffidi, M. White and A. G. Williams, Phys. Rev. D **92** (2015) no.10, 103519 [arXiv:1502.02667 [hep-ph]].
- [59] G. S. Bali *et al.* [QCDSF Collaboration], Phys. Rev. Lett. **108** (2012) 222001 [arXiv:1112.3354 [hep-lat]].
- [60] P. Junnarkar and A. Walker-Loud, Phys. Rev. D **87** (2013) 114510 [arXiv:1301.1114 [hep-lat]].
- [61] P. Bechtle, O. Brein, S. Heinemeyer, O. Stl, T. Stefaniak, G. Weiglein and K. E. Williams, Eur. Phys. J. C **74** (2014) no.3, 2693 [arXiv:1311.0055 [hep-ph]].
- [62] P. Bechtle, S. Heinemeyer, O. Stl, T. Stefaniak and G. Weiglein, Eur. Phys. J. C **74** (2014) no.2, 2711 [arXiv:1305.1933 [hep-ph]].
- [63] R. R. de Austri, R. Trotta and L. Roszkowski, JHEP **0605**, 002 (2006) [hep-ph/0602028].
- [64] J. R. Ellis, T. Falk, K. A. Olive and M. Srednicki, Astropart. Phys. **13** (2000) 181 Erratum: [Astropart. Phys. **15** (2001) 413] [hep-ph/9905481].
- [65] M. E. Gomez, G. Lazarides and C. Pallis, Phys. Rev. D **61** (2000) 123512 [hep-ph/9907261].
- [66] C. Boehm, A. Djouadi and M. Drees, Phys. Rev. D **62** (2000) 035012 [hep-ph/9911496].
- [67] S. Mizuta and M. Yamaguchi, Phys. Lett. B **298** (1993) 120 [hep-ph/9208251].
- [68] J. Edsjo and P. Gondolo, Phys. Rev. D **56** (1997) 1879 [hep-ph/9704361].
- [69] S. Profumo and C. E. Yaguna, Phys. Rev. D **69** (2004) 115009 [hep-ph/0402208].
- [70] D. Feldman, Z. Liu and P. Nath, Phys. Rev. D **80** (2009) 015007 [arXiv:0905.1148 [hep-ph]].
- [71] U. Chattopadhyay, D. Choudhury, M. Drees, P. Konar and D. P. Roy, Phys. Lett. B **632** (2006) 114 [hep-ph/0508098].
- [72] I. Gogoladze, S. Raza and Q. Shafi, JHEP **1203** (2012) 054 [arXiv:1111.6299 [hep-ph]].
- [73] I. Gogoladze, R. Khalid, S. Raza and Q. Shafi, JHEP **1012** (2010) 055 [arXiv:1008.2765 [hep-ph]].
- [74] I. Gogoladze, F. Nasir, Q. Shafi and C. S. Un, Phys. Rev. D **90** (2014) no.3, 035008 doi:10.1103/PhysRevD.90.035008 [arXiv:1403.2337 [hep-ph]].
- [75] <http://www.xenon1t.org/>
- [76] CMS collaboration, <https://twiki.cern.ch/twiki/bin/view/CMSPublic/PhysicsResultsSUS>.
- [77] H. Okawa [ATLAS Collaboration], arXiv:1110.0282 [hep-ex].
- [78] S. Chatrchyan *et al.* [CMS Collaboration], Phys. Rev. D **88** (2013) no.5, 052017 [arXiv:1301.2175 [hep-ex]].
- [79] F. Ambrogio *et al.*, Comput. Phys. Commun. **227** (2018) 72 [arXiv:1701.06586 [hep-ph]].
- [80] M. Drees, H. Dreiner, D. Schmeier, J. Tattersall and J. S. Kim, Comput. Phys. Commun. **187** (2015) 227 [arXiv:1312.2591 [hep-ph]].

- [81] N. Arkani-Hamed, P. Schuster, N. Toro, J. Thaler, L. T. Wang, B. Knuteson and S. Mrenna, hep-ph/0703088 [HEP-PH].
- [82] S. Kraml, S. Kulkarni, U. Laa, A. Lessa, W. Magerl, D. Proschofsky-Spindler and W. Waltenberger, Eur. Phys. J. C **74** (2014) 2868 doi:10.1140/epjc/s10052-014-2868-5 [arXiv:1312.4175 [hep-ph]].
- [83] F. Ambrogio, S. Kraml, S. Kulkarni, U. Laa, A. Lessa and W. Waltenberger, Eur. Phys. J. C **78** (2018) no.3, 215 [arXiv:1707.09036 [hep-ph]].
- [84] P. Z. Skands *et al.*, “SUSY Les Houches accord: Interfacing SUSY spectrum calculators, decay packages, and event generators,” JHEP **0407** (2004) 036 [hep-ph/0311123].
- [85] T. Sjöstrand *et al.*, Comput. Phys. Commun. **191** (2015) 159 doi:10.1016/j.cpc.2015.01.024 [arXiv:1410.3012 [hep-ph]].
- [86] A. Djouadi, M. M. Muhlleitner and M. Spira, Acta Phys. Polon. B **38** (2007) 635 [hep-ph/0609292].
- [87] <http://phystev.in2p3.fr/wiki/2013:groups:tools:slha>.
- [88] A. M. Sirunyan *et al.* [CMS Collaboration], Phys. Rev. D **96** (2017) no.3, 032003 [arXiv:1704.07781 [hep-ex]].
- [89] A. M. Sirunyan *et al.* [CMS Collaboration], Eur. Phys. J. C **77** (2017) no.10, 710 [arXiv:1705.04650 [hep-ex]].
- [90] G. Aad *et al.* [ATLAS Collaboration], JHEP **1409** (2014) 176 [arXiv:1405.7875 [hep-ex]].
- [91] A. M. Sirunyan *et al.* [CMS Collaboration], JHEP **1710** (2017) 005 [arXiv:1707.03316 [hep-ex]].
- [92] A. M. Sirunyan *et al.* [CMS Collaboration], Phys. Rev. D **97** (2018) no.1, 012007 [arXiv:1710.11188 [hep-ex]].
- [93] A. M. Sirunyan *et al.* [CMS Collaboration], JHEP **1710** (2017) 019 [arXiv:1706.04402 [hep-ex]].
- [94] A. M. Sirunyan *et al.* [CMS Collaboration], JHEP **1803** (2018) 160 [arXiv:1801.03957 [hep-ex]].